Article ID: 1003－6326(2003)04－0794－04

Effect of heat-treatment on fatigue property of Al-Li alloy①

ZHANG Di(张 荻), DING Jian(丁 剑), FAN Tong-xiang(范同祥),
LÜ Wei-jie(吕维洁), QIN Ji-ning(覃继宁)
(State Key Laboratory of Metal Matrix Composites, Shanghai Jiaotong University,
Shanghai 200030, China)

Abstract: Fatigue property of Al-Li alloy after various heat treatment was investigated. The results show that the fatigue strength is enhanced with the age hardening progressing. Compared to the solution treated specimen, the fatigue limit is improved to 136% for sub-ageing treated specimen and 155% for peak-ageing treated specimen, respectively. In the meanwhile, the fatigue deformation becomes non-uniform with age hardening progressing. The fatigue cracks initiate and propagate prior from the uni-uniform slip band, causing transgranular fracture or the mixed mode of transgranular fracture and intergranular fracture.

Key words: Al-Li alloy; heat treatment; fatigue property
CLC number: V 25; TG 115.31 **Document code:** A

1 INTRODUCTION

More than 80% of structural materials' failures are caused by fatigue failure directly or indirectly.[1, 2] Al-Li alloy has been used as a kind of new structural space flight material because of its high strength and low density.[3, 4] Although a lot of researches about Al-Li alloy[5-8] have been done in the past few years, the detailed study on the fatigue property[9-10] has not been done so much. Especially, there was little research on the fatigue crack initiating and propagating behavior. Because the strength of Al-Li alloy could be affected effectively by the ageing treatment, the fatigue property of Al-Li alloy after various ageing treatment is investigated in this work.

2 EXPERIMENTAL

The pure Al (> 99.99%) and pure Li (99.96%) were melt at 800 ℃ in Al_2O_3 crucible in which the melted metal was protected with Ar gas. Then, Al-Li alloy cast ingot was made by being cast into an iron mold. The chemical composition of cast ingot was analyzed and shown in Table 1.

Table 1 Chemical composition of tested Al-Li alloy (mass fraction, %)

Li	Fe	Cu	Mg	K	Al
1.82	0.003 9	0.009 4	0.000 7	0.003 1	Bal.

The cast ingots were uniformly treated at 570 ℃ for 24 h with Ar gas protection. Then, the surface layer of cast ingot was removed by machining. Then, 2.3 mm thick board was made by proper cold and hot roller working. The specimens were cut along the roller working direction. After being solution treated at 500 ℃ for 1 h, the specimens were quenched into ice water immediately, then they were ageing treated under 3 kinds of conditions in oil furnace, and called respectively as type A specimen (solution treatment), type B specimen (sub ageing treatment at 150 ℃, 24 h) and type C specimen (peak ageing treatment at 150 ℃, 500 h), respectively.

The fatigue test was done with UF-15 Shimatsu fatigue testing machine (Stress ratio $R = -1$, $f = 30$ Hz). The fatigue limit was defined as the fatigue strength when the cycle number reached 10^7. The microstructure was observed and analyzed with Olympus Optical Microscope and Hitachi X-650S SEM. The grain size was measured by using Line Truncation Method. The fractographic analysis was done with Hitachi X-650S SEM.

3 RESULTS AND DISCUSSIONS

3.1 Fatigue strength of Al-Li alloy affected by heat treatment

The high cycle fatigue test was done by using three kinds of typical heat treated specimens mentioned above. The fatigue test results are shown in Fig. 1. The same fatigue test of the pure Al (> 99.99%) was also done in order to compare the fatigue property of the pure Al. Fig. 1 shows that, the fatigue strength of Al is improved obviously by adding

① **Foundation item:** Project (G19999064907-6) supported by the State Key Fundamental Research and Development Program of China
Received date: 2003－01－10; **Accepted date:** 2003－03－26
Correspondence: ZHANG Di, Professor, PhD; Tel: +86-21-62933106; Fax: +86-21-62822012; E-mail: Zhangdi@sjtu.edu.cn

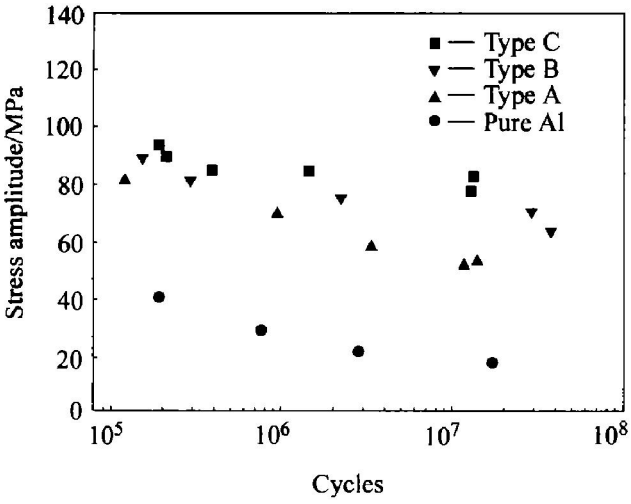

Fig. 1 Fatigue strength of pure Al and Al-1.8% Li alloys

Li even at the solution treatment state. Furthermore, the fatigue strength increases gradually with increasing ageing time.

Fig. 2 shows the change of the hardness of alloy with the increasing of ageing time. The hardness increases in initial stage with extending ageing time, and reaches the peak when the ageing time reaches around 500 h. These results match the experimental results shown in Fig. 1 very well.

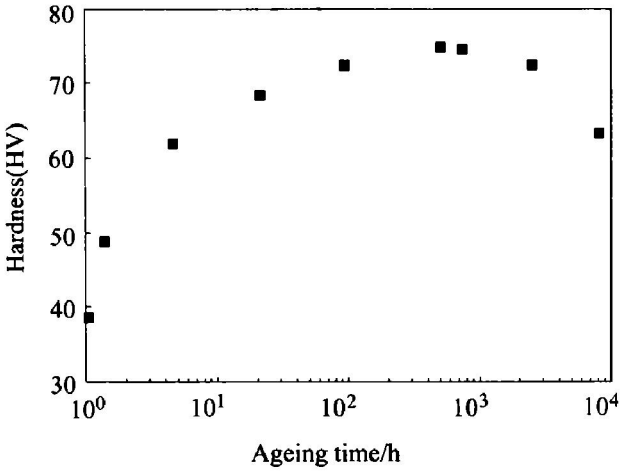

Fig. 2 Change of hardness with ageing time for Al-1.8% Li alloy

3.2 Initiation and propagation behavior of fatigue cracks

Fig. 3 shows the surface observation result of type A specimen during the fatigue test. Comparatively uniform slip bands inside the grain are observed in the initial fatigue stage. Those slip bands penetrated the whole grain shown in Fig. 3(a). The straight line slip bands with around 1.5 μm gap width are observed shown in Fig. 3(b) at higher magnification. Some of the above mentioned slip bands become coarser with increasing fatigue cycles as shown in Fig. 3(c). Then, the fatigue cracks initiate along

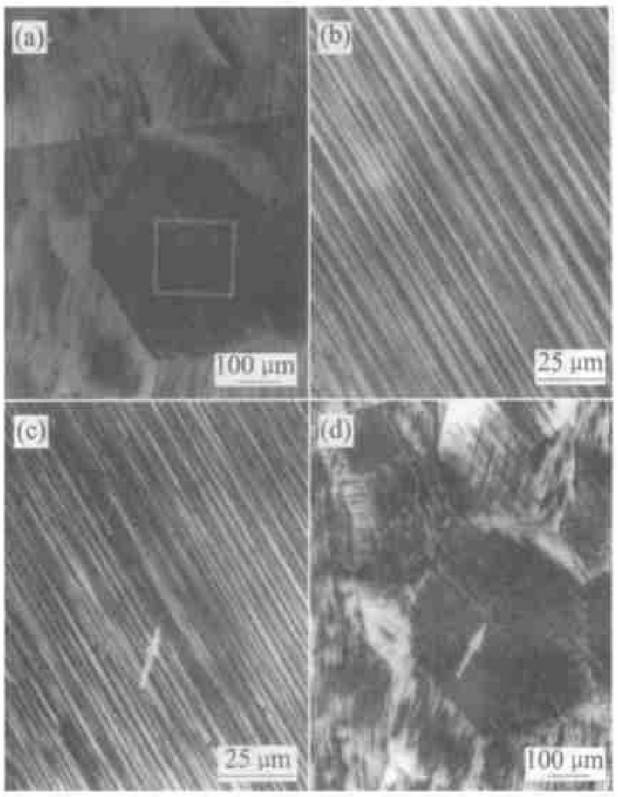

Fig. 3 Surface observation micrographs of type A specimen during fatigue test at different fatigue cycles ($\sigma_a = \pm 56$ MPa)
(a) $-N = 3.0 \times 10^3$; (b) $-N = 3.0 \times 10^3$;
(c) $-N = 5.1 \times 10^6$; (d) $-N = 7.1 \times 10^6$

those coarse slip bands and propagates inside the grain, inducing the fatigue fracture finally.

Fig. 4 shows the surface observation micrograph of type B specimen during the fatigue test. The number of the slip bands inside the grain decreases obviously compared to type A specimen. The inhomogeneous deformation occurred as shown in Fig. 4(a). The fatigue cracks initiated along the inhomogeneous slip bands and propagates. Finally they induces the fatigue fracture as explained in Figs. 4(b), (c) and (d).

Fig. 5 shows the surface observation micrograph of type C specimen in the fatigue test. Compared to Figs. 3 and 4, it is observed that, more rare slip bands generate inside the grain in the initial fatigue stage. The fatigue cracks initiate along the slip bands and the grain boundary, while the fatigue cracks inside the grain are much easier to propagate transgranularly which is indicated with the arrow in Fig. 5. It seems that the fatigue crack inside the grain was much easier to become the fatal crack inducing the fatigue fracture finally. It is considered that the inhomogeneous deformation occurs much easier inside the grain due to the ageing strengthening. Furthermore, the stress concentration degree increases with the number of the slip bands reducing.

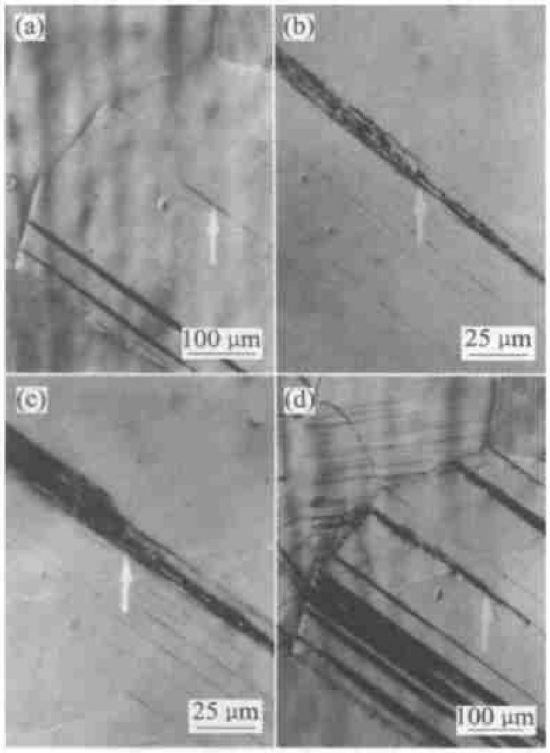

Fig. 4 Surface observation micrographs of type B specimen at different fatigue cycles with $\sigma_a = \pm 92$ MPa
(a) —$N = 2.3 \times 10^3$; (b) —$N = 1.5 \times 10^4$; (c) —$N = 5.0 \times 10^4$; (d) —$N = 5.0 \times 10^4$

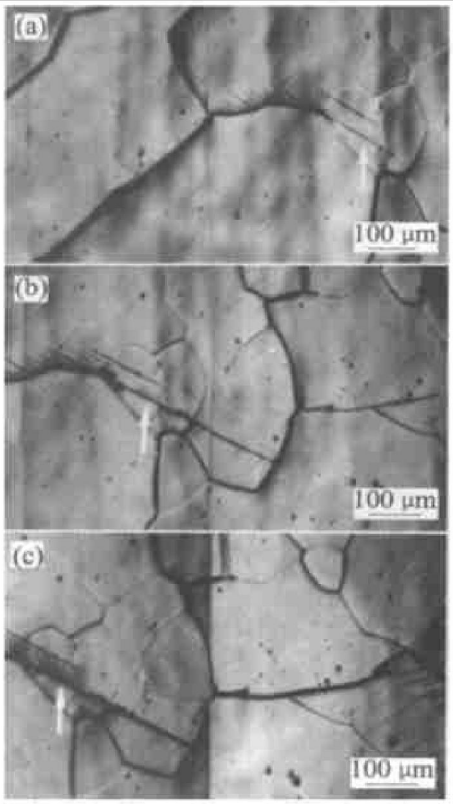

Fig. 5 Surface observation of micrographs of type C specimen at different fatigue cycles with $\sigma_a = \pm 92$ MPa
(a) —$N = 7.0 \times 10^4$; (b) —$N = 1.0 \times 10^5$; (c) —$N = 1.2 \times 10^5$

3.3 Fractography of fatigue fracture

Fig. 6(a) shows the entire transgranular fracture of type A specimen. Fractography of type B specimen shows almost transgranular fracture, although sometimes the intergranular fracture is observed. All the above observations match the successive observation of the fatigue initiation and propagation behavior indicated in Section 3.2. Fig. 6(b) shows the fatigue fracture of type C specimen. It often shows the mixed mode combined by the transgranular and intergranular fracture. Compared to the observation shown in Fig. 6(a), the fracture surface is smoother, and the coplanar slip step is observed clearly.

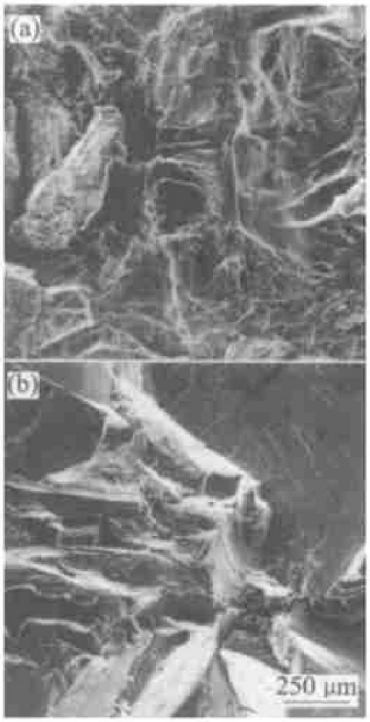

Fig. 6 Fractographs of fatigue fracture
(a) —Type A specimen, $\sigma_a = \pm 59$ MPa, $N = 3.31 \times 10^4$; (b) —Type C specimen, $\sigma_a = \pm 84$ MPa, $N = 1.5 \times 10^6$

3.4 Age hardening mechanisms induced by precipitation of δ′

The fatigue property was obviously enhanced by the age hardening of δ′ phase. Therefore, it was necessary to discuss its strengthening mechanism. The alloy after peak ageing treatment was chosen as the example, and the strengthening mechanisms are discussed as follows.

1) Effect of lattice mismatch between δ′ and matrix (τ_a) could be calculated by[11]

$$\tau_a = 11.8 G_m \varepsilon^{3/2} r_s^{1/2} b^{-1/2} f^{5/6} \quad (1)$$

where f is volume fraction of δ′, 0.06[12]; G_m is shear modulus of matrix, 28.2 GPa[13]; ε is lattice mismatch between δ′ and matrix, 0.1%[13]; r_s is average radius of δ′ on slip planes, $r_s = (2/3)^{1/2} r_0$, r_0 is average radius of measured δ′, usually fixed as 180; b is burgers vector, 2.86×10^{-10} m;

2) Effect of the shear modulus difference be-

tween δ' and matrix (τ_b) could be calculated by[13]

$$\tau_b = \frac{\delta G}{4\pi^2}\left[\frac{3\delta G}{G_m b}\right]^{1/2} \cdot \left[0.8 - 0.143\ln\left(\frac{r_s}{b}\right)\right]^{3/2} (r_s f)^{1/2} \quad (2)$$

where δG is shear modulus difference between δ' and the matrix, G of δ' was calculated as 34.3 MPa from the measurement[13].

3) The surface between δ' and the matrix increased after the dislocation cutting the δ' particle. The total surface energy was increased. The effect of surface energy could be calculated by[13]

$$\tau_c = \frac{\sqrt{6}}{\pi} r_s f \sigma^1 \quad (3)$$

where σ is surface energy between δ' and matrix, 0.014 J/m^2[14]

4) The border upon relation between Li atom and Al atom in δ' particle was changed when the dislocation cutting the δ' particle. The antiphase boundary was generated. The effect of antiphase boundary could be calculated by[13]

$$\tau_d = \frac{\gamma}{2b}\left[\left[\frac{4\gamma r_s f}{\pi T}\right]^{1/2} - f\right] \quad (4)$$

$$\frac{\pi T f}{4\gamma} < r_s < \frac{T}{\gamma}$$

where T is line tension of the dislocation, let $T = G_m b^2/2$; γ is antiphase boundary energy.

The above strengthening effects are calculated and summarized in Table 1.

Table 1 Strengthening effect from various mechanisms

Type	Equation	Age strengthening effect/MPa
(a)	(1)	5.2
(b)	(2)	25.3
(c)	(3)	0.04
(d)	(4)	26.3

According to the above calculation, it was considered that the age strengthening effect was chiefly induced by (b) and (d).

Supposed the dislocation passes the δ' particle by rounding method instead of cutting method, the needed critical stress could be calculated by

$$\tau_e = \frac{G_m b}{2\pi l}\ln\left(\frac{2r_s}{r_c}\right) \quad (5a)$$

$$\tau_s = \frac{\tau_e}{1-\nu} \quad (5b)$$

where l is average clearance between δ' particles, $l = [(\pi/f)^{1/2} - 2] \times r_s$; r_c is radius of dislocation core, 2.86×10^{-10} m; ν is 0.4;

By calculation it can be obtained that: τ_e = 77.7 MPa, τ_s = 130 MPa. The stress for the dislocation cutting δ' particles is lower than that for the dislocation rounding δ' particles. So, it could be considered the fatigue deformation was induced by the dislocation cutting the δ' phase.

REFERENCES

[1] Nishida S. Failure Analysis in Engineering Applications [M]. London: Butterworth Heinemann Co Ltd, 1992. 4.

[2] DING Jian, Nishida S, Hattori N. Effect of strain aging and overstress on fatigue property of SUS304[J]. Transactions of JSME, A, 2000, 66: 1331 - 1336. (in Japanese)

[3] XIA De-shun. The application and analysis of new light alloys in aerospace vehicle (1) [J]. Missiles and Space Vehicles, 2000, 4: 18 - 22. (in Chinese)

[4] XIA De-shun. Technological research of tank structural material for launch vehicle (2) [J]. Missiles and Space Vehicles, 1999, 3: 32 - 41. (in Chinese)

[5] Chen D L, Chaturvedi M C. Effects of welding and weld heat-affected zone simulation on the microstructure and mechanical behavior of a 2195 aluminum-lithium alloy [J]. Metall Mater Trans A, 2001, 32(11): 2729 - 2741.

[6] Ciupinski L, Mizera J, Kurzydlowski K J. Quantitative description of the morphologic texture in an Al-Li alloy [J]. Mater Charact, 2001, 46(5): 359 - 364.

[7] Kwon Y N, Koh H J, Lee S, et al. Effects of microstructural evolution on superplastic deformation characteristics of a rapidly solidified Al-Li alloy[J]. Metall Mater Trans A, 2001, 32(7): 1649 - 1658.

[8] Potti P K G, Rao B N, Srivastava V K. Residual strength of aluminum-lithium alloy center surface crack tension specimens at cryogenic temperatures[J]. Cryogenics, 2000, 40(12): 789 - 795.

[9] Lewandowska M, Mizera J, Wyrzykowski J W. Cyclic behaviour of mode Al-Li alloys: effect of the precipitate state[J]. Mater Charact, 2000, 45(3): 195 - 202.

[10] Kobayashi T. Strength and fracture of aluminum alloys [J]. Materials Science and Engineering A, 2000, 280(1): 8 - 16.

[11] Gleiter H, Hornbogen E. Theorie der wechselwirkung von versetzungen[J]. Physica Status Solidi A, 1965, 12: 235 - 250. (in German)

[12] Kouda N. Transmission Electron Microscopy [M]. Tokyo, Korona Press, 1974. 480. (in Japanese)

[14] Noble B, Harris S J, Dinsdahl K. Yield characteristics of aluminium-lithium alloys[J]. Metal Science, 1982, 16: 425 - 430.

[15] Bavmann S F, Willams D B. A new method for the determination of the precipitate-matrix interfacial energy [J]. Scripta Metallurgica, 1984, 18: 611 - 616.

(Edited by LONG Huai-zhong)